Journal of Atmospheric Chemistry **46:** 239–269, 2003.

On the Drop-Size Dependence of Organic Acid and Formaldehyde Concentrations in Fog

B. ERVENS [1⋆], P. HERCKES [2], G. FEINGOLD [3], T. LEE [2], J. L. COLLETT, JR. [2] and S. M. KREIDENWEIS [2]

[1] *Cooperative Institute for Research in the Atmosphere (CIRA), Colorado State University, Fort Collins, Colorado 80523, U.S.A.*
[2] *Atmospheric Science Department, Colorado State University, Fort Collins, CO 80523, U.S.A.*
[3] *NOAA, Environmental Technology Laboratory, Boulder, Colorado 80305, U.S.A.*

(Received: 15 May 2003; accepted: 28 July 2003)

Abstract. Concentration differences between small ($r < 8.5$ μm) and large droplets ($r > 8.5$ μm) were observed for formic acid, acetic acid and formaldehyde in fog droplets collected in California's Central Valley. The concentration ratios (large/small droplets) of these compounds were investigated by a stepwise model approach. Assuming thermodynamic equilibrium (K_H^{eff}) results in an overestimate of the concentration ratios. Considering the time dependence of gas phase diffusion and interfacial mass transport, it appears that the lifetime of fog droplets might be sufficiently long to enable phase equilibrium for formaldehyde and acetic acid, but not for formic acid (at pH $\approx$7). Oxidation by the OH radical has no effect on formaldehyde concentrations but reduces formic acid concentrations uniformly in all drop size classes. The corresponding reaction for acetic acid is less efficient so that only in large droplets, where replenishment is slowed because the uptake rate of acid from the gas phase is slower, is the acid concentration reduced leading to a smaller concentration ratio. Formaldehyde concentrations in fog can be higher than predicted by Henry's Law due to the formation of hydroxymethanesulfonate. Its formation is dependent on the sulfur(IV) concentration. At high pH values the uptake rate for sulfur(IV) is drop-size dependent. However, the observed concentration ratios for formaldehyde cannot be fully explained by the adduct formation. Finally, it is estimated that mixing effects, i.e., the combination of individual droplets into a bulk sample, have a minor influence (<15%) on the measured heterogeneities.

Key words: aqueous phase chemistry, fog, formaldehyde, modelling, organic acid, uptake.

1. Introduction

Organic acids and formaldehyde have been detected in high concentrations in fog (e.g., Winiwarter *et al.*, 1994; Millet *et al.*, 1997; Collett *et al.*, 1999a) and in cloud droplets (e.g., Keene *et al.*, 1995; Hegg *et al.*, 2002; Löflund *et al.*, 2002). Organic acids in fog droplets may be derived through particle or gas phase scavenging. Species with low vapor pressures (such as dicarboxylic acids), predominately associated with the atmospheric particulate phase, are contributed mainly from cloud

⋆ Address for correspondence: NOAA/ETL, 325 Broadway, Boulder, Colorado 80305, U.S.A., e-mail: barbara.ervens@noaa.gov

condensation nuclei. Dicarboxylic acids are typically found in submicron particles (Neusüß *et al.*, 2000; Yao *et al.*, 2002).

The partitioning of volatile species (such as HCOOH, CH_3COOH and HCHO) between gas and aqueous phases depends on their solubility. The available surface area affects the uptake rate but not the equilibrium partitioning. Simultaneous measurements of gas and aqueous phase concentrations are sparse. In a few studies (e.g., Winiwarter *et al.*, 1994; Voisin *et al.*, 2000) it has been shown that equilibrium between the phases is not achieved. A partition coefficient represents the deviation from equilibrium. Partition coefficients greater than unity indicate that the droplets are supersaturated with respect to gas phase concentrations. For HCOOH and CH_3COOH partition coefficients between 0.001 and 40 have been found (Leriche *et al.*, 2000). In the presence of sulfur(IV), formaldehyde can form the adduct hydroxymethanesulfonate (HMS^-). Measured concentrations of formaldehyde in droplets usually include the concentration of this adduct. Therefore, the observed partitioning of formaldehyde can exceed significantly that predicted by Henry's Law (Ang *et al.*, 1987; Olson and Hoffmann, 1989). Concentrations of both formaldehyde and sulfur(IV) in droplets have been observed to be higher by factors of up to 100 and 1000, respectively, than predicted by their Henry's Law constants (Klippel and Warneck, 1980; Ang *et al.*, 1987).

Measurements of solute concentrations in cloud and fog droplets have been analyzed in several studies and often show higher solute concentrations in small droplets (Pandis *et al.*, 1990; Ogren *et al.*, 1992; Collett *et al.*, 1994; Bator and Collett, 1997; Reilly *et al.*, 2001). One contribution to such concentration differences might be that the uptake rates of soluble gases vary for droplets of different sizes. Mass transfer from the gas phase can lead to drop size-dependent uptake rates (Audiffren *et al.*, 1998), while fast chemical reactions within the aqueous phase can also prevent attainment of equilibrium. In addition to these effects, mixing of single droplets into a bulk sample might result in a different equilibrium concentration than present originally in the individual droplets (Pandis and Seinfeld, 1991; Khare *et al.*, 1999). Each of these effects has been addressed in the studies mentioned above, but to date there has been no evaluation of the relative contribution of each effect to observed deviations from equilibrium between the aqueous and gas phases.

In the present study observations are presented of low molecular weight organic compounds in fog. Concentrations of mono- and dicarboxylic acids and formaldehyde are found to vary with drop size. Different hypotheses are examined to explain these observations for formic acid, acetic acid and formaldehyde. An uptake/chemistry model is used to interpret differences in the partitioning between the gas and aqueous phases for these three species. Based on these model results, a more general view of the contributions to deviations from phase equilibrium for transport, chemistry and drop mixing effects is developed.

2. Experimental

2.1. INSTRUMENTATION

Fog samples were collected in December 2000 and January 2001, close to the small town of Angiola (N35°35′, W119°32′, 60 m asl) in the Central Valley of California, as part of the California Regional Particulate Air Quality Study (CRPAQS). In this study, radiation fogs usually formed at night and evaporated in the early morning hours. Samples were typically collected at one hour intervals. Drop size distribution spectra were recorded by a Classical Scattering Active Spectrometer Probe (CSASP, Particle Measurement Systems Inc.).

Fog Liquid Water Content (LWC) was monitored at the site using a Particle Volume Monitor (Gerber Scientific, PVM-100). Fog samples for Total Organic Carbon (TOC) and organic acid analyses were collected with stainless steel versions of the Caltech Active Strand Cloudwater Collector (ss-CASCC) and a two-stage version of that collector known as the size-fractionating ss-CASCC (sf-ss-CASCC) (Herckes *et al.*, 2002a). The 50% size cuts of the two sf-ss-CASCC stages are estimated as approximately $r = 3$ μm and $r = 8.5$ μm. Collection efficiency curves for the cloud collector stages have an S-shape. While the size cut of the small drop stage is fairly sharp, the collection efficiency curve for the large drop stage is flatter (Demoz *et al.*, 1996), covering a span of several μm while rising from low to high collection efficiency. These metal collectors can be cleaned with solvents in order to reduce contamination by organic compounds. Samples for formaldehyde analysis were collected with plastic versions of the CASCC and sf-CASCC (Demoz *et al.*, 1996), collocated and operated simultaneously with the metal collectors. Possible contamination was checked with field blanks, taken before fog events.

Immediately after sample collection, the pH value of each sample was measured. Organic acid aliquots were stabilized by addition of chloroform as a biocide and kept refrigerated in the dark until analysis (Wortham *et al.*, 1995 and references therein). Analysis was completed within 4 weeks after the end of the field project. Formic, acetic, propionic, oxalic, pyruvic, malonic and succinic acids were determined by ion chromatography using a Dionex DX500 system equipped with a Dionex AS11-HC column and guard column, a Dionex ATC-1 Anion trap column and a Dionex CD20 conductivity detector. Elution was performed with a sodium hydroxide gradient as follows: start to 8 minutes: 4 mM NaOH; then the NaOH concentration was progressively increased: 15 mM at 23 minutes; 30 mM at 28 minutes; 60 mM at 38 minutes.

Formaldehyde was preserved by reaction with buffered sulfur(IV) to form hydroxymethanesulfonate. This was later dissociated and reacted with 2,4-pentanedione to form 3,5-diacetyl-1,2-dihydrolutidine, which was analyzed by fluorescence (Dong and Dasgupta, 1987). The excitation wavelength used was 412 nm and the emission wavelength 510 nm. This technique allows for total formaldehyde measurement but does not allow for a differentiation between free formaldehyde and hydroxymethanesulfonate.

Table I. Concentrations of small mono and dicarboxylic acids and formaldehyde in bulk fog droplets (μeq/L)

	Monocarboxylic acids/formaldehyde			
	Formaldehyde HCHO	Formic HCOOH	Acetic CH_3COOH	Propionic CH_3CH_2COOH
Minimum	<DL	14.9	5	<DL
Median	21.5	31.6	31.4	<DL
Maximum	43.9	121	197	10.4
Average	23.4	42.1	51.4	–
DL = detection limit	*3.3*	*4.2*	*4.1*	*3.7*
	Dicarboxylic acids			
	Oxalic $(COOH)_2$	Malonic $HO_2CCH_2CO_2H$	Succinic $HO_2C(CH_2)CO_2H$	Glutaric $HO_2C(CH_2)_3CO_2H$
Minimum	<DL	<DL	<DL	<DL
Median	7.19	<DL	<DL	<DL
Maximum	24.8	5.17	<DL	6.92
Average	8.4	–	–	–
DL = detection limit	*3.2*	*5.0*	*5.8*	*5.6*

Total Organic Carbon (TOC) concentrations were determined using a commercial TOC analyzer (Shimadzu TOC 5000A), which oxidizes organic carbon in an injected sample on a catalyst bed at 680 °C, followed by measurement of the evolved carbon dioxide. The TOC analyzer was calibrated using a series of aqueous potassium hydrogen phthalate standards; measurement precision was evaluated through replicate sample analyses.

2.2. BULK FOG WATER CONCENTRATIONS

Table I gives an overview of observed concentrations of mono- and dicarboxylic acids as well as formaldehyde in bulk fog samples. Measured formaldehyde concentrations represent the sum of free formaldehyde, formaldehyde present in solution in its gem-diol form, and hydroxymethanesulfonate. For the monocarboxylic acids, formic acid and acetic acid concentrations are similar while propionic acid concentrations are much lower, sometimes even undetectable. Dicarboxylic acids are frequently undetectable (<5 μeq/L), with the exception of oxalic acid, which shows concentrations in the range of half of formic acid concentrations.

Table II. Average (minimum-maximum) concentrations of formic, acetic and oxalic acids and formaldehyde measured in different studies (μM)

Location	Formic acid	Acetic acid	Oxalic acid	Formaldehyde	Reference
Radiation fogs					
Angiola (SJV, Ca)	**42 (15–121)**	**51 (5–197)**	**4.2 (<1.6–12)**	**23 (3–44)**	**This study**
Bakersfield (SJV, Ca)	77 (40–167)	83 (0–244)		168 (27–498)	Munger *et al.*, 1989a
McKittrick (SJV, Ca)	21 (0–56)	3 (0–28)		26 (6–93)	Munger *et al.*, 1989a
Visalia (SJV, Ca)	71 (40–187)	86 (35–187)		31 (18–65)	Munger *et al.*, 1989a
Buttonwillow (SJV, Ca)	145 (133–157)	60 (47–74)		88 (61–115)	Munger *et al.*, 1989a
San Joaquin Valley (Ca)	63 (6–270)	117 (10–458)	6.2 (<2.7–16.5)	46.4 (2.3–410)	Collett *et al.*, 1999a
Po Valley (Italy)	9.5–165.5	12.5–91.5			Winiwarter *et al.*, 1988
Po Valley (Italy)				130 (16–567)	Facchini *et al.*, 1990
Strasbourg (France)	110 [a]/190 [b]	305 [a]/440 [b]		n.d.	Millet *et al.*, 1997
Clouds					
Mt. Rax (Austria)	13 (1–34)	16 (11–37)	4.2 (0.7–12.7)		Löflund *et al.*, 2002
Whiteface Mt. (U.S.A.)	26 (14–40)	9 (5.1–15)	5.25 (1.5–9.5)		Khwaja *et al.*, 1995
San Pedro Hill (Ca)	20 (12–43)	10 (6–31)		13 (5–38)	Munger *et al.*, 1989b

[a] 5–8 μm droplets.
[b] 2–6 μm droplets, n.d. not determined.

Table II presents the range of observations for formic and acetic acid as well as formaldehyde in selected studies. While several data sets exist for these three compounds, published data on other mono- and dicarboxylic acids in cloud and fog droplets are sparse. In previous studies in California's San Joaquin Valley (SJV), Munger *et al.* (1989a, b) determined concentrations of organic acids and formaldehyde similar to those found in the current study. The urban Visalia and Bakersfield sites showed higher concentrations than the rural Angiola sampling site, while the remote McKittrick site showed lower values. Observations from 1989 in the small town of Buttonwillow showed much higher values, but these observations are based on only two samples. In a composite of urban and remote San Joaquin Valley sites, with a large number of samples collected in urban areas (Fresno and Bakersfield), Collett *et al.* (1999a) found higher concentrations than observed in the present study. The Angiola concentrations are also of the same order of magnitude as found in Po Valley radiation fogs (Winiwarter *et al.*, 1988). In the urban environment of Strasbourg higher concentrations were observed in very small droplets (2 to 6 μm or 5 to 8 μm in diameter) by Millet *et al.* (1996, 1997). Finally, observations in intercepted clouds in Europe and in the United States usually exhibit lower concentrations of acetic and formic acid and formaldehyde than are observed in fogs. Oxalic acid concentrations measured in intercepted clouds in Austria and the U.S. were similar to those observed in polluted radiation fogs in the San Joaquin Valley.

2.2.1. *Contributions of Low Molecular Weight Organic Compounds to the Total Organic Carbon (TOC)*

The total organic carbon (TOC) concentrations in this study ranged from 2 to 40 ppmC. Usually more than 50% of the organic matter consisted of low molecular weight compounds (<500 g/mol) (Herckes *et al.*, 2002a). Figure 1 gives an overview of the contributions of low molecular weight carboxylic acids and formaldehyde to TOC. On average these compounds account for 22% of the fog TOC. Monocarboxylic acids contribute the most to the total organic carbon, accounting for an average of 17% of the TOC. Acetic acid is usually the dominant organic species, accounting for up to 22% of the TOC, while formic and propionic acids contribute less (up to 10 and 2%, respectively). The concentration of pyruvic acid is usually less than 0.1% of the TOC. The dicarboxylic acids investigated account for only 1% of the TOC on average. Oxalic acid is most important; concentrations of the higher dicarboxylic acids are one order of magnitude smaller. Formaldehyde accounts for 4% of the TOC on average. Concentrations of other carbonyls (e.g., acetaldehyde or glyoxal) were not determined in this study. Previous studies by Munger *et al.* (1990) revealed that glyoxal and methylglyoxal concentrations were in the same concentration range as formaldehyde and hence may provide similar contributions to TOC.

The results here are consistent with studies of fog samples in Davis, CA (Herckes *et al.*, 2002b) where acetic acid was also the dominant organic species. In the more urban environment of Davis, however, acetic and formic acid accounted

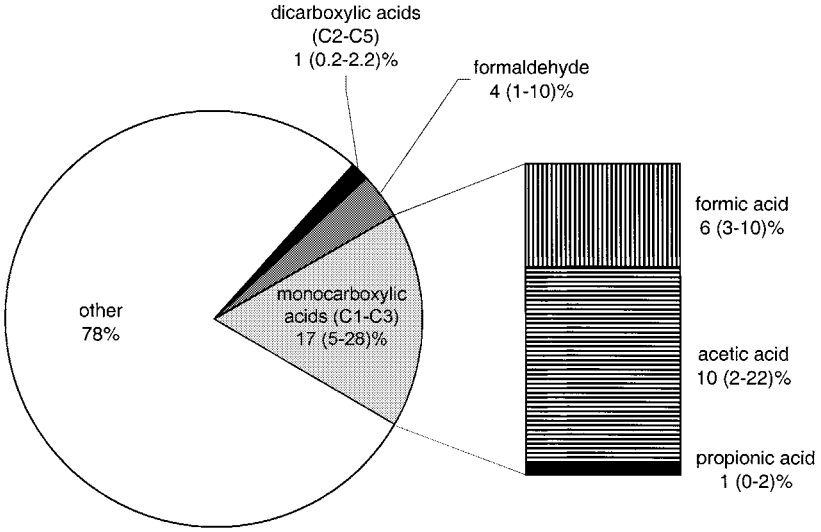

Figure 1. Average (min-max) contributions of formaldehyde, mono- and dicarboxylic acids to the Total Organic Carbon in Angiola fog samples (in % of TOC).

for only 11% of the TOC on average. Similar observations have been made by Löflund (2002) in clouds at Mt. Rax in Austria, where small organic acids accounted for 11% of the OC on average (5–22%) and the dicarboxylic acids only accounted for 1.7% on average.

2.3. VARIATION OF CONCENTRATIONS WITH DROPLET SIZE

The collection of size-fractionated samples enables a comparison between concentrations in small droplets (3 μm $< r <$ 8.5μm) and large droplets ($r >$ 8.5μm). Figures 2(a–c) present the observations for low molecular weight acids (formic, acetic, propionic and oxalic acid) and formaldehyde. In general, the small droplets exhibit higher concentrations than the large droplets. Propionic acid does not follow this trend as clearly as the other acids, but few observations are available. Such observations of chemical heterogeneity have already been made for inorganic compounds in radiation fogs (e.g., Millet *et al.*, 1996; Bator and Collett, 1997; Laj *et al.*, 1998) as well as for total organic carbon (Herckes *et al.*, 2002b). Munger and coworkers (1989b) observed little difference in formate, acetate and formaldehyde concentrations between small and large droplets in cloud samples collected at San Pedro Hill (CA). Keene *et al.* (1995) reported making drop size-resolved measurements of organic acid concentrations but did not report results. Millet and coworkers (1997) observed enrichment in smaller droplets in a study investigating two size classes of small droplets (2–6 μm and 5–8 μm in diameter).

Chemical heterogeneity in drop composition has sometimes been explained by the chemical heterogeneity of the aerosol population on which these droplets form

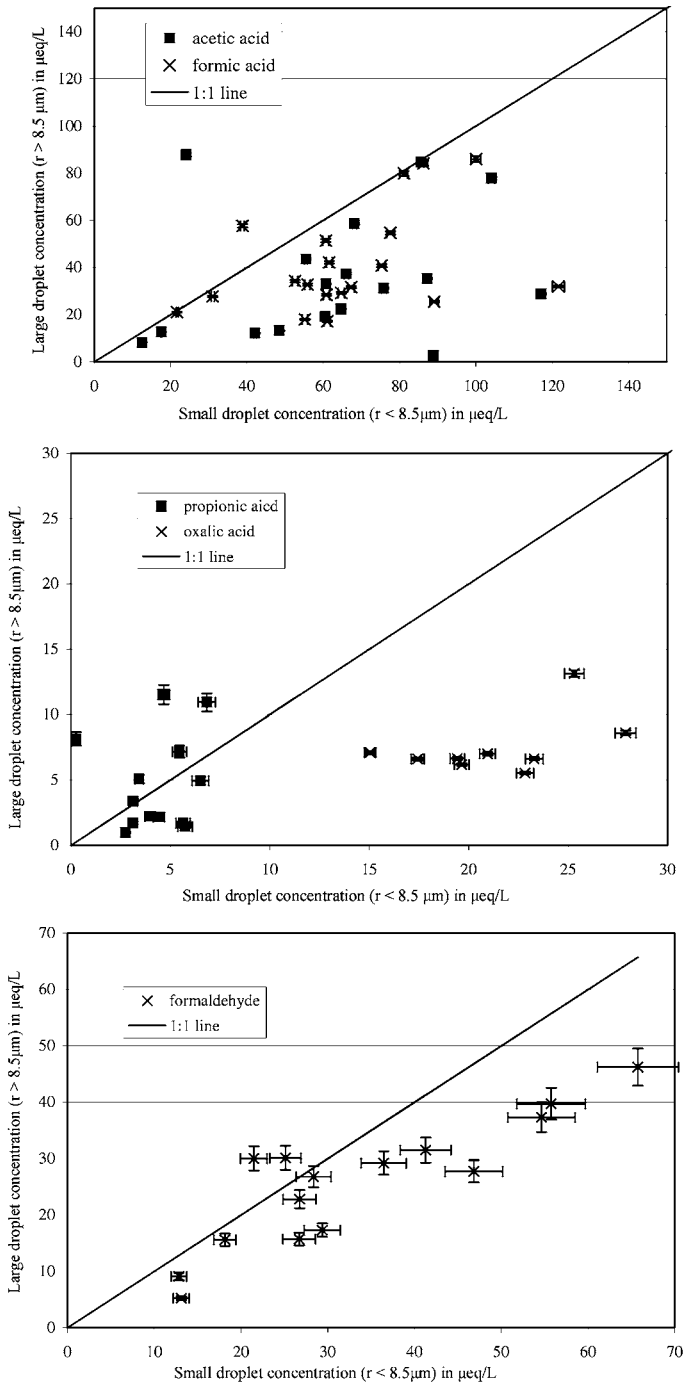

Figure 2. Concentrations in small vs. large droplets in Angiola, California radiation fogs. Error bars represent the measurement precision (one relative standard deviation) associated with sample analysis. (a) Formic and acetic acid; (b) propionic and oxalic acid; (c) formaldehyde.

(Ogren and Charlson, 1992; Bator and Collett, 1997). Smaller cloud condensation nuclei, which typically produce smaller drops, usually show higher concentrations of organic carbon, sulfate and ammonium. Larger fog drops are likely to form on larger condensation nuclei, formed by mechanical processes, which might be relatively enriched in sodium, chloride and calcium.

These relations might not fully explain observed conditions (i) because the dilution of aerosol material in the droplets also influences the concentrations and (ii) because droplet growth depends on aerosol composition. In size resolved aerosol studies, it was shown that oxalic and other dicarboxylic acids are mainly found in the accumulation mode (Ludwig and Klemm, 1988; Neusüß *et al.*, 2000). Hence, the higher concentrations of oxalate (Figure 2(b)) in the smaller droplets can be explained by the enrichment of oxalate in the smaller condensation nuclei.

This explanation, however, cannot account for the observations of formic acid, acetic acid and formaldehyde, as these low molecular weight organic compounds have a high vapor pressure and are found predominately in the gas phase rather than in particles. These compounds are incorporated into fog droplets through gas phase scavenging and, therefore, nucleation scavenging of aerosol particles does not play a significant role in their distribution with drop size. The review by Yu (2000) shows that in most cases roughly 1% of these acids are present in the aerosol phase if no liquid water is present. In a model study by Herrmann *et al.* (2000) it has been shown that under urban conditions (pH < 4) the aqueous phase fractions of these species can increase to about 8% for both acids and more than 90% for formaldehyde. However, the partitioning is strongly dependent on the available liquid water content and the pH value. Under less polluted conditions (i.e., higher pH values) the aqueous phase fractions of the acids will increase significantly. In the following section, possible reasons will be discussed for the observed concentration inhomogeneities of formic acid, acetic acid and formaldehyde in different droplet size classes.

3. Modeling

3.1. THERMODYNAMIC EQUILIBRIUM: HENRY'S LAW

The equilibrium phase partitioning of slightly soluble and less reactive gases can be described by the ratio of the aqueous phase concentration c_{aq} and the gas phase partial pressure p, as expressed by the Henry's Law Constant $\mathrm{K_H}$ [M atm^{-1}]

$$\mathrm{K_H} = \frac{c_{\mathrm{aq}}[\mathrm{M}]}{p\ [\mathrm{atm}]}\,. \tag{1}$$

Dissociation of acids in the aqueous phase increases their effective solubility. For this reason the effective Henry's Law Constant $\mathrm{K_H}^{\mathrm{eff}}$, including the dissociation constant K_a, is applied for acids:

$$\mathrm{K_H^{eff}(acids)} = \mathrm{K_H} \cdot \left(1 + \frac{\mathrm{K}_a}{[\mathrm{H^+}]}\right). \tag{2}$$

For aldehydes, such as formaldehyde, the hydration (hydration constant K_{Hydr}) within the aqueous phase must be taken into account:

$$K_H{}^{eff}(\text{aldehydes}) = K_H \cdot \left(1 + K_{hydr} \cdot [H_2O]\right) . \quad (3)$$

However, the application of Henry's Law constants might not be appropriate if aqueous solutions with high ionic strengths are present. In addition to organic acids, concentrations of inorganic ions (SO_4^{2-}, NO_3^-, Cl^-, NO_2^-, Mg^{2+}, Ca^{2+}, Na^+, K^+ and NH_4^+) were determined in the fog droplets. For most of these ions higher concentrations were found in smaller droplets. However, the total ionic strength in both the large and small droplets did not exceed a value of $I = 0.001$ M so that ionic strength effects on the Henry's Law Constants ('salting out effects') can be neglected here. At equilibrium the monocarboxylic acids and formaldehyde should have the same concentrations in all droplet size classes (assuming the same effective solubility, i.e., the same pH value in the case of the acids).

$$\text{ratio} = \frac{\text{concentration in large droplets [M]}}{\text{concentration in small droplets [M]}} . \quad (4)$$

Observations typically reveal significantly lower pH values in small droplets (e.g., Bator and Collett, 1997); however, in the present study this trend was not clearly observed. Only small differences between the pH values of small droplets (average 7.02, range 6.43–7.75) and large droplets (7.04, 6.2–7.74) were observed. At these high pH values, the ratio $K_a/[H^+]$ is always much greater than 1 (pK_a (HCOOH) = 3.75, pK_a (CH_3COOH) = 4.75) and Equations (2) and (4) can be combined to yield

$$\text{ratio} = \frac{[A^-]_{large}}{[A^-]_{small}} = \frac{[H^+]_{small}}{[H^+]_{large}} . \quad (5)$$

In Figure 3 the measured concentration ratios of formate and acetate are compared to the values predicted by Equation (5). It is evident that in some cases there is good agreement between the measured and the predicted values; however, in most cases the measured ratio is lower than expected for equilibrium phase partitioning. This result, along with the observations for formaldehyde in Figure 2(c), suggests that the actual partitioning of these three species might not have achieved equilibrium and other effects should be considered.

3.2. KINETIC DESCRIPTION OF MASS TRANSFER

Henry's Law describes the equilibrium solubility without any consideration of the time scales of the uptake process. However, as shown by Schwartz (1986) the uptake rate is a time dependent process controlled by several factors, including gas phase diffusion, interfacial mass transfer, aqueous phase diffusion and chemical reactions within the aqueous phase. The reciprocal value of the rate [s^{-1}] of each

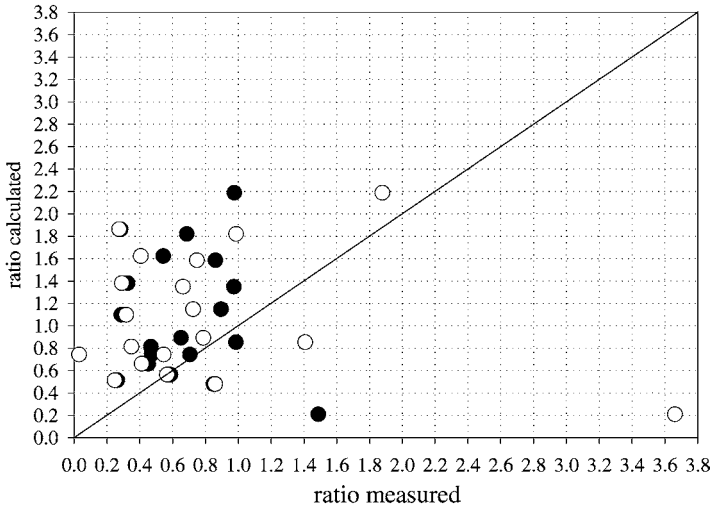

Figure 3. Comparison of measured concentration ratios (large/small drops) and predicted ratios based on the effective Henry's Law Constants for ● formic and O acetic acid.

process can be defined as a characteristic time. A comparison of these characteristic times allows the determination of the rate-limiting process. In the following sections each of these factors will be investigated to clarify its possible contribution to the observed concentration inhomogeneities.

3.2.1. *Gas Phase Diffusion and Interfacial Mass Transfer*

The uptake rate is dependent on the rate of transport from the gas phase. Transport slows with decreasing concentration gradients between the bulk gas phase and the droplet surface. The combination of these two factors yield the uptake rate [M s^{-1}] in terms of the time rate of change of the aqueous phase surface concentrations

$$\frac{d\,[c]_{\mathrm{aq}}}{dt} = k_{\mathrm{mt}} \cdot p - \frac{[c]_{\mathrm{aq}}}{\mathrm{K_H}^{(\mathrm{eff})} \cdot \mathrm{R} \cdot \mathrm{T}}\,, \tag{6}$$

where k_{mt} is the mass transfer coefficient [s^{-1}]. k_{mt} can be calculated according to the approach by Schwartz (1986)

$$k_{\mathrm{mt}} = \left[\left(\frac{r^2}{3 \cdot \mathrm{D}_g} + \frac{r}{4 \cdot \bar{c} \cdot \alpha}\right)\right]^{-1}\,, \tag{7}$$

where r is the drop radius, D_g the gas phase diffusion coefficient, $\bar{c}$ the molecular speed $(8 \cdot \mathrm{R}' \cdot \mathrm{T}/(\pi \cdot \text{molar mass}))^{0.5}$ (where R′ is the gas constant in [J $(\mathrm{K} \cdot \mathrm{mol})^{-1}$]) and

$$\alpha = \frac{\text{No. of molecules entering the liquid phase}}{\text{No. of molecular collisions with the surface}}\,. \tag{8}$$

The reciprocal value of the mass transfer coefficient (7), multiplied by the (dimensionless) Henry's Law Constant $K_H^{(eff)} \cdot R \cdot T$, represents the characteristic time for achieving equilibrium at the drop surface. In the absence of aqueous phase reactions, if further transport through the droplet interior is sufficiently rapid this time scale describes the characterisitc time until the whole drop is saturated with the surrounding gas. In the model study by Warneck (1999) it was shown that the uptake rate on droplets of $r = 5\ \mu$m is on the order of $k_{mt} = 10^5\ s^{-1}$ for soluble gases ($K_H(eff) > 30\ M\ atm^{-1}$). In the present study the concentration ratios of the three species of interest in the aqueous phase were calculated applying Equation (6), combined with Equation (7), using the uptake parameters for formic acid, acetic acid and formaldehyde (Table III). The concentrations in the gas phase were estimated to be 0.1 ppb. They were held constant for the simulation. The choice of the gas phase concentration does not have any influence on the final ratio if a fixed pH value is assumed as done here. The analytical solution of (6) for the fixed-pH, fixed-gas-phase case reveals that the concentration ratio is always independent of the partial pressure, as can be seen from the following

$$c_{aq}(t) = -(K_H^{(eff)} \cdot R \cdot T) \cdot \exp(-t \cdot k_{mt}/(K_H^{(eff)} \cdot R \cdot T)) + (K_H^{(eff)} \cdot R \cdot T) \cdot p. \quad (9)$$

Thus, the concentration ratio can be determined as

$$\begin{aligned} \frac{c_{aq,\,1}}{c_{aq,\,2}} &= \frac{-(K_H^{(eff)} \cdot R \cdot T) \cdot p \cdot \exp(-t \cdot k_{mt,\,1}/(K_H^{(eff)} \cdot R \cdot T)) + (K_H^{(eff)} \cdot R \cdot T) \cdot p}{-(K_H^{(eff)} \cdot R \cdot T) \cdot p \cdot \exp(-t \cdot k_{mt,\,2}/(K_H^{(eff)} \cdot R \cdot T)) + (K_H^{(eff)} \cdot R \cdot T) \cdot p} \\ &= \frac{1 - \exp(-t \cdot k_{mt,\,1}/(K_H^{(eff)} \cdot R \cdot T))}{1 - \exp(-t \cdot k_{mt,\,2}/(K_H^{(eff)} \cdot R \cdot T))} \end{aligned} \quad (10)$$

which is independent of the partial pressure. Corresponding measurements of gas phase concentrations are not available from the current study, but the estimate seems to be appropriate leading to aqueous phase concentrations comparable to the measured values. Calculations were performed for pH values between 6 and 8, covering the limits in the present study.

The evolution of the resulting concentration ratios over 30 min, a typical fog drop lifetime, is shown in Figure 4 for formic acid and acetic acid. At the beginning of the simulation time the acid concentrations in the droplets correspond to the ratio of the k_{mt} values. Thus, the axis intercept of about 0.45 is due to this ratio. Saturation is achieved for acetic acid after about 30 min at pH = 7. The timescale for formic acid to reach equilibrium is much longer, because due to its higher effective solubility, about ten times more molecules must be transported towards the droplet surface. In previous studies the lifetime of fog droplets was assumed to range from a few minutes to hours (Noone *et al.*, 1992; Winiwarter *et al.*, 1994). This means that within the lifetime of a fog droplet, acetic acid is more likely to reach equilibrium in the droplet than formic acid. The uptake rate for formaldehyde is not shown in the figure as it is almost independent of the pH value and equilibrium is reached after about 10 s. (The more sophisticated approach

Table III. Uptake parameters for formic acid, acetic acid, formaldehyde and OH

	$K_{H,\,298\,K}$ [M atm^{-1}]	$\Delta H/R$ [K]	K_a [M]	$\Delta H/R$ [K]	$\alpha_{298\,K}$	$\alpha_{279\,K}$	D_g [m^{-2} s^{-1}]	
HCOOH	5530	–5630 [a]	$1.77 \cdot 10^{-4}$	–12 [d]	0.012 [f]	0.035 [g]	$1.53 \cdot 10^{-5}$ [h]	$1.45 \cdot 10^{-9}$ [j]
CH_3COOH	5500	–5890 [b]	$1.75 \cdot 10^{-5}$	–46 [d]	0.019 [f]	0.05 [g]	$1.24 \cdot 10^{-5}$ [h]	$1.29 \cdot 10^{-9}$ [j]
HCHO	2.5	–7216 [b]	36	–4030 [e] *	0.02 **	0.02	$1.64 \cdot 10^{-5}$ [i]	$1.64 \cdot 10^{-9}$ [k]
OH	25	–5280 [c]			0.05 **	0.05	$1.53 \cdot 10^{-5}$ [j]	$1.53 \cdot 10^{-9}$ [k]

[a] Khan and Brimblecombe, 1992; [b] Betterton and Hoffmann 1988; [c] Kläning *et al.*, 1985; Harned and Owen, 1958; * K_{Hydr} [M^{-1}]; [d] Olson and Hoffmann, 1989; [e] Davidovits *et al.*, 1995; [f] Nathanson *et al.*, 1996; ** estimated, therefore no T dependence available; [g] Schwartz, 1986; [h] estimated based on the method by Fuller, 1986; [i] Hanson *et al.*, 1992; [j] Lide *et al.*, 2000; [k] estimated $D_g = 10^4 \cdot D_{aq}$.

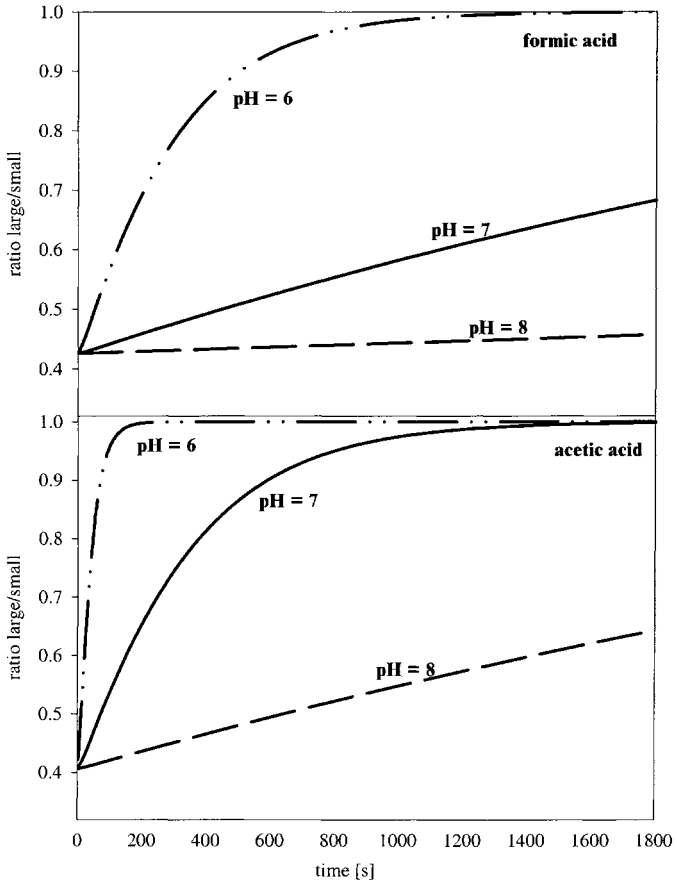

Figure 4. Predicted ratio (concentration in large/small droplets; $r = 12\ \mu$m, $r = 6\ \mu$m) in absence of chemical reactions for formic (upper panel) and acetic acid depending on the time and pH of the aqueous phase $- \cdot \cdot - \cdot$ pH = 6; ——— pH = 7; - - - - - pH = 8.

considering the pH dependence of the formaldehyde uptake as suggested by Swartz *et al.* (1997) is neglected here due to the small variation of the uptake rate between pH = 4 and 10). But if one assumes a lifetime of the fog droplets of several minutes it can be seen (Figure 4) that this simple model, which considers only the uptake kinetics, would not predict for the same time similar concentration ratios for both acids of 0.6 ± 0.25 (mean value of the measured ratios $\pm$ standard deviation) as found in the measurements.

The characteristic time until achievement of equilibrium $(k_{\mathrm{mt}})^{-1}$ represents the sum of the characteristic times for the gas phase diffusion τ_{gdiff} and the time for the interfacial transport $\tau_{\mathrm{interfacial}}$.

$$\tau_{\mathrm{gdiff}} = \frac{r^2}{3 \cdot \mathrm{D}_g} \cdot \mathrm{K}_{\mathrm{H}}^{(\mathrm{eff})} \cdot \mathrm{R} \cdot \mathrm{T} \tag{11}$$

$$\tau_{\text{interfacial}} = \frac{4 \cdot r}{3 \cdot \alpha \cdot \overline{c}} \cdot \mathrm{K}_{\mathrm{H}}^{(\mathrm{eff})} \cdot \mathrm{R} \cdot \mathrm{T}. \tag{12}$$

In addition to the characteristic time associated with the overall mass transfer coefficient these individual characteristic times are shown in Figure 5. In small droplets the interfacial transport processes control the uptake of gases, whereas for larger droplets the transport towards the droplet surface, i.e., the gas phase diffusion, is slower (Figure 5). The radius (r_{limit}) at which the interfacial limitation is surpassed by diffusion limitation is different for the three species ($r_{\text{limit}}(CH_3COOH) \approx 3.5\ \mu$m; $r_{\text{limit}}(HCOOH) \approx 5.5\ \mu$m; $r_{\text{limit}}(HCHO) \approx 7.5\ \mu$m), but for all of them this crossover fits into the observed 'small droplets' category ($r < 8.5\ \mu$m). Therefore, the uptake in the large droplets is always more strongly limited by gas phase diffusion.

One reason for the disagreement between observed and predicted concentration ratios might be the uncertainty in the mass accommodation coefficient. It is known that mass accommodation coefficients show slight temperature dependence due to the decreasing energy barrier to enter the droplet surface with decreasing temperature (Nathanson *et al.*, 1996). This temperature dependence is opposite to that of the Henry's Law Constant but is much weaker. The average temperature measured during the fog events was approximately 279 ($\pm$7) K. In this range the mass accommodation coefficients might be enhanced by a factor of 2 compared to the values at 298 K (Nathanson *et al.*, 1996).

The mass accommodation coefficients in Table III are values for pure water surfaces. At enhanced ionic strengths the mass accommodation coefficients are lower. However, the low ionic strengths present in the fog droplets will not significantly change the coefficients applied here.

On small droplets in the atmosphere, the mass accommodation coefficients could be significantly smaller due to organic hydrophobic coatings on the droplet surfaces (Gill *et al.*, 1986). The presence of such films may slow penetration of the surface and therefore increase the limitation of the uptake processes by interfacial transfer. Measurements of film forming compounds such as fatty acids ($>C_{12}$) in fog droplets are available (e.g., Herckes *et al.*, 2002b). Assuming an average value based on those data it appears that there is insufficient film forming organic material to form a monolayer on the droplets throughout the size distribution from 2 to 47 μm (diameter). However, the presence of organic films in the initial stages of fog droplet formation might lead to a retardation of the droplet growth leading finally to a concentration inhomogeneity in droplets of the same size (Podzimek and Saad, 1975; Feingold and Chuang, 2002). For film forming species, higher concentrations were found in smaller particles (Neusüß *et al.*, 2000), so that smaller droplets within the measured size distribution might be preferentially coated. Due to the lack of more detailed sets of size resolved data a more exact estimate cannot be given here.

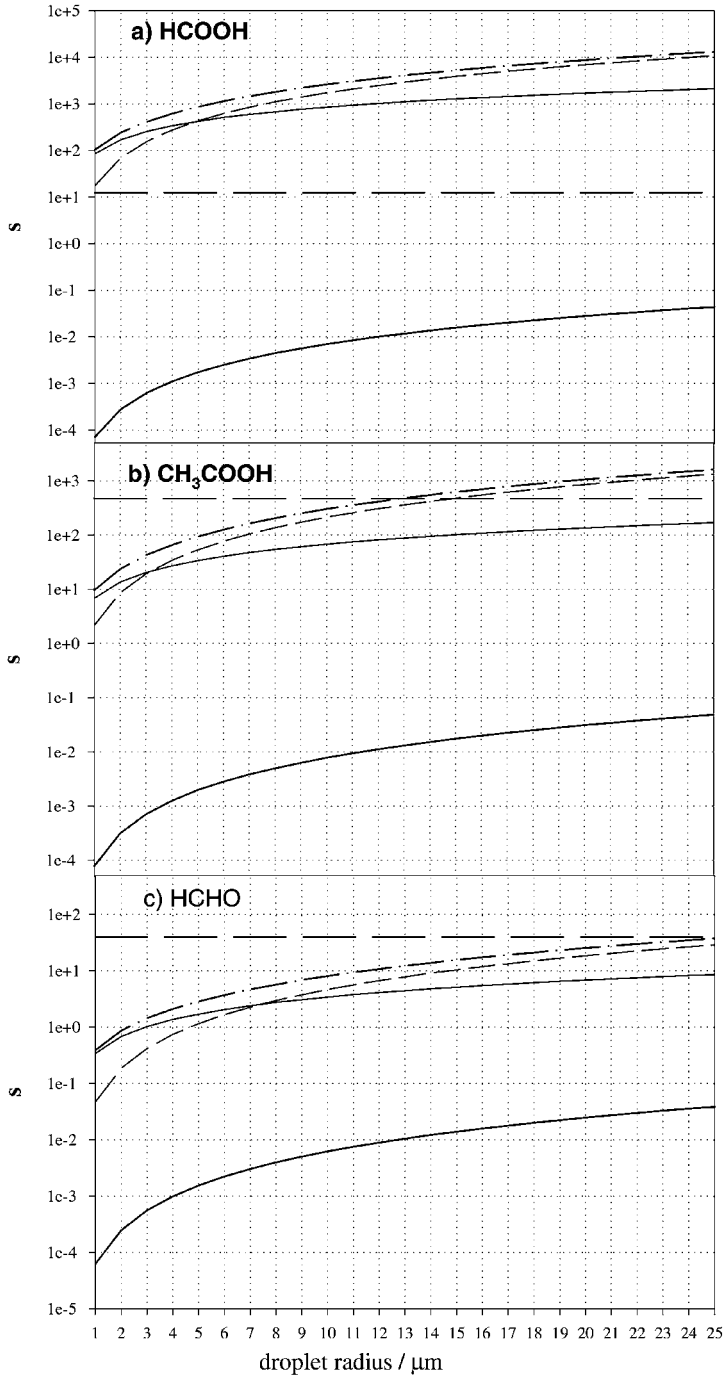

Figure 5. Characteristic times for interfacial mass transfer $\tau_{interfacial}$ ———; gas phase diffusion τ_{gdiff} – – – –; — · — $\tau_{gdiff} + \tau_{interfacial}$ (= time until thermodynamic equilibrium is achieved at drop surface); aqueous phase diffusion τ_{aqdiff} chemical reaction τ_{reac} ——— and – – – –.

3.2.2. *Aqueous Phase Diffusion*

The model equation (6) used in Section 3.2.1 refers to the equilibrium concentration at the droplet surface. In the next step of the model development we investigate if there are concentration gradients between the droplet surface and the droplet interior. Gradients will occur if the diffusion within the droplet is slow compared to the transport from the gas phase. The characteristic time for the aqueous phase diffusion τ_{aqdiff} [s] is given by Equation (13) (Schwartz, 1986).

$$\tau_{\mathrm{aqdiff}} = \frac{r^2}{\pi^2 \cdot D_{\mathrm{aq}}} . \tag{13}$$

The time scale for the aqueous phase diffusion is always significantly shorter than that for the mass transfer from the gas phase ($\tau_{\mathrm{gdiff}} + \tau_{\mathrm{interfacial}}$) (Figure 5). Hence, for the species of interest here the aqueous phase diffusion is fast enough to provide a homogeneous concentration profile through the droplet, in the absence of chemical reaction.

More generally, the crossover between gas phase and aqueous phase mass transport limitations has been derived using different theoretical approaches (Schwartz, 1986; Huthwelker and Peter, 1996). For example, the expression by Schwartz (1986)

$$\mathrm{K_H^{(eff)}} > \frac{1}{5 \cdot \mathrm{R} \cdot \mathrm{T}} \frac{\mathrm{D}_g}{\mathrm{D_{aq}}} \tag{14}$$

is based on the assumption that the concentrations in both the gas and aqueous phase might deviate by 10% from their respective equilibrium concentrations. Therefore, for less soluble species aqueous phase diffusion might be the rate limiting process. Using Equation (14), a limit solubility can be estimated at which the limitation by aqueous phase transport gains in importance. Assuming a ratio of $\mathrm{D}_g/\mathrm{D_{aq}} \approx 10^{-4}$ (cf. Table III) at a temperature of 279 K the aqueous phase diffusion is only limiting for species with $\mathrm{K_H^{(eff)}} \leqslant 90$ M atm^{-1}. However, for the highly soluble species investigated in the present study the effective solubility is greater than this minimum by a few orders of magnitude.

3.3. CHEMICAL PROCESSES IN THE AQUEOUS PHASE

The discussion above shows that ($\tau_{\mathrm{gdiff}} + \tau_{\mathrm{interfacial}}$) represents the characteristic time for the droplets to approach saturation with the gases and achieve the concentrations predicted by the Henry's Law constants. But this equilibrium might be disturbed by the consumption of the species of interest by chemical reactions. Schwartz (1986) showed that equilibrium is not reached in the droplets if the timescale for chemical reaction τ_{chem}

$$\tau_{\mathrm{chem}} = (k \cdot [\mathrm{reactant}])^{-1} \tag{15}$$

is approximately ten times less than that for aqueous phase diffusion, τ_{aqdiff}. The fastest aqueous phase reactions for the three species considered in this study are the oxidation by radicals. Recently it has been shown that oxidation of organic compounds in the aqueous phase can be adequately described by reactions with the OH radical (Ervens *et al.*, 2003). Even at night the contributions of the NO_3 radical to oxidation in the aqueous phase are less important due to OH production within the droplets by light-independent sources.

In addition to chemical processes in the bulk aqueous phase, there is evidence that surface processes might take place at the interface between gas and droplet (e.g., Nathanson *et al.*, 1996). But current knowledge of those processes is too limited to implement reliable values into models (Worsnop *et al.*, 2002).

The model was extended to include the uptake of $OH_{(g)}$ described in the same way as for the acids, using appropriate uptake parameters (Table III). Gas phase concentrations of $[OH]_{g,\text{day}} = 10^7$ cm^{-3} and $[OH]_{g,\text{night}} = 10^4$ cm^{-3} were assumed. These concentrations were chosen as reasonable upper limits in order to estimate the maximum likely effect of chemical reactions and give an upper bound for this mechanism. However, if a lower, more moderate, initial gas phase concentration is assumed the characteristic time for chemical reaction in the aqueous phase will be even longer so that at least for acetic acid and formaldehyde the importance of the OH reaction in controlling the aqueous phase concentration is even smaller. The radical concentration was kept constant during the simulation. This is a reasonable simplification for the simulation period of 30 min ($\approx$ lifetime of fog droplets). Of course, the same considerations for the uptake process made for the acids are also applicable for the OH radical, but its solubility is much lower so that the transport limitation into the droplet is smaller. In addition to the time scales for the transport processes, the characteristic times for the OH reaction are shown in Figure 5. These characteristic times are independent of the drop radius and they are represented by the horizontal (broken) lines in all three figures, respectively. It is assumed that for the short simulation times the OH concentration is constant and the term $k \cdot [\text{reactant}]$ can be simplified to a first order rate constant $k^{1\text{st}}$ based on an OH concentration $[OH]_{\text{aq}} = 3 \cdot 10^{-11}$ M and the rate constants given in Table V. (This OH concentration is based on the 'day time' OH concentration; the corresponding value for 'night time' would be smaller by three orders of magnitude.)

A measure of the effectiveness of aqueous phase diffusion compared to the time scale for the chemical reaction is given by the diffuso-reactive parameter

$$q = r \cdot \sqrt{\frac{k^{1\text{st}}}{\text{D}_{\text{aq}}}}. \tag{16}$$

As explained by Schwartz (1986) values of $q > 1$ correspond to a significant depletion of the species by the chemical processes and lead to a decreasing penetration of the species towards the drop center. The values of q are shown in Table IV for all three species. They are all significantly smaller than 1 indicating a uniform reaction rate throughout the drop. This result also confirms the applicability of

Table IV. Characteristic times [s] for gas phase diffusion, interfacial mass transfer, aqueous phase diffusion and chemical reactions within the aqueous phase and diffuso-reactive parameter q

	r/μm	τ_{gdiff}	τ_{interfac}	$(\tau_{\text{gdiff}} + \tau_{\text{interfacial}}) \cdot K_H \cdot R \cdot T$	τ_{aqdiff}	τ_{chem} (OH reaction)	
HCOOH	1	$2 \cdot 10^{-8}$	$1.5 \cdot 10^{-7}$	104	$6.2 \cdot 10^{-5}$	0.08	0.0074
	10	$2 \cdot 10^{-6}$	$1.5 \cdot 10^{-6}$	2633	$6.2 \cdot 10^{-3}$	0.08	0.074
CH_3COOH	1	$2.2 \cdot 10^{-8}$	$1 \cdot 10^{-7}$	13	$6.6 \cdot 10^{-5}$	0.002	0.0012
	10	$2.2 \cdot 10^{-6}$	$1 \cdot 10^{-6}$	336	$6.6 \cdot 10^{-3}$	0.002	0.012
HCHO	1	$2.7 \cdot 10^{-8}$	$8.5 \cdot 10^{-8}$	0.03	$8.2 \cdot 10^{-5}$	0.025	0.0043
	10	$2.7 \cdot 10^{-6}$	$8.5 \cdot 10^{-7}$	0.8	$8.2 \cdot 10^{-3}$	0.025	0.043

the assumption that aqueous phase diffusion processes are fast enough to ensure a well-mixed drop interior.

3.3.1. *Formic and Acetic Acid*

In Figure 6 the concentration ratios for the acids predicted by the time-dependent reactive transport model approach are presented. It is evident that nighttime chemistry does not significantly influence the concentration ratios in the fog droplets, so that the predictions cannot be differentiated from the results from the 'pure' uptake model (Figure 4; pH = 7). On the other hand, it is evident that during daytime, the ratios can be influenced significantly by the oxidation of the acids and values similar to those observed are predicted for a range of droplet lifetimes. The ratios are very sensitive to the assumed OH concentration. Measured concentrations are not available but the OH concentrations assumed here give reasonable lower and upper limits for the possible influence of chemical loss processes.

From Figure 6, one can see that formic acid aqueous phase concentrations will reach steady state, but will never be in equilibrium due to the fast consumption by OH. The difference between τ_{chem} and $(\tau_{\text{gdiff}} + \tau_{\text{interfacial}})$ is smallest for small droplets (Figure 5). Thus, the concentrations in large droplets will be more affected by chemical processes than those in small ones, leading to a decrease in the ratio. Qualitatively the same argument is valid for acetic acid, but here most of the drops are not significantly affected by reaction so that drops of radius < 15 μm might approach thermodynamic equilibrium with a timescale of $(\tau_{\text{gdiff}} + \tau_{\text{interfacial}})$. In summary, the concentration ratio is more strongly affected by reaction of OH for acetic acid despite a much smaller rate constant. However, the absolute acid concentrations will be decreased more for formic acid.

Jacob (1986) has also discussed implications of the formation of these acids by the oxidation of their corresponding precursors by OH. Formic acid is effec-

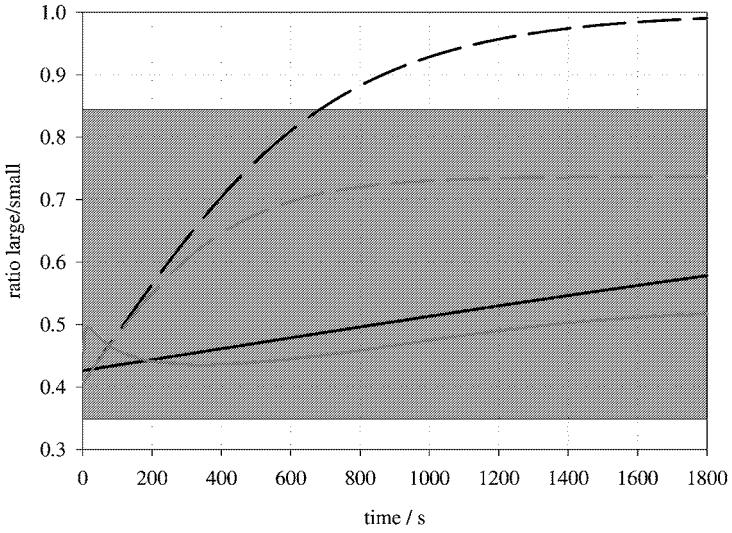

Figure 6. Concentration ratios for formic and acetic acid with chemical loss processes within the aqueous phase (pH = 7); shadowed area: measured ratios (average ± standard deviation); grey lines: daytime; black lines: nighttime); solid line: HCOOH, broken line: CH_3COOH.

tively produced by the oxidation of formaldehyde, leading to an accumulation or even outgassing of formic acid. However, under the conditions found here (pH $\approx$ 7) formic acid is completely dissociated ($pK_a = 3.75$). The oxidation of formate by OH is about 25 times faster than that of formic acid and formaldehyde ($k_{HCOO^-} = 3.2 \cdot 10^9$ M^{-1} s^{-1}; $k_{HCOOH} = 1.2 \cdot 10^8$ M^{-1} s^{-1}; $k_{CH_2(OH)2} = 7.7 \cdot 10^8$ M^{-1} s^{-1}). Therefore, the further oxidation of formate is too fast to allow it to accumulate. The corresponding formation process for acetic acid from acetaldehyde is much less important because (1) the gas phase concentration of acetaldehyde is usually found to be lower than formaldehyde (Saxena and Hildemann, 1996) and (2) the effective solubility (K_H^{eff}) is lower due to a smaller hydration constant of acetaldehyde (Betterton and Hoffmann, 1988). Therefore, the main sources of acetic acid are gas phase processes.

3.3.2. *Formaldehyde*

The oxidation of (hydrated) formaldehyde in the aqueous phase represents the main known sink for the OH radical within droplets. Formaldehyde can form the sulfur(IV) adduct hydroxymethanesulfonate (HMS^-), which is less reactive with radicals than free formaldehyde and less reactive with other oxidants, such as H_2O_2 and O_3 than sulfite or bisulfite. As pointed out in 2.2.1. the measured formaldehyde concentration includes both free and hydrated formaldehyde as well as HMS^-.

The oxidation of $CH_2(OH)_2$ by OH, the formation of HMS^- and the oxidation of this adduct by OH were added to the model (Table V). Furthermore, to avoid

Table V. Rate/equilibrium constants of chemical processes of formic and acetic acid and formaldehyde within the aqueous phase

Reaction	k or K	$-\Delta H/R$	Reference
$OH + HCOO^- \rightarrow$ products	$3.2 \cdot 10^9\ M^{-1}\ s^{-1}$	1000	Chin and Wine, 1994
$OH + CH_3COO^- \rightarrow$ products	$1 \cdot 10^8\ M^{-1}\ s^{-1}$	1800	Chin and Wine, 1994
$HCHO_{(g)} \rightleftharpoons CH_2(OH)_{2(aq)}$	$4998\ M\ atm^{-1}$	4030	Betterton and Hoffmann, 1988
$SO_{2(g)} \rightleftharpoons SO_{2(aq)}$	$1.24\ M\ atm^{-1}$	3247	Beilke and Gravenhorst, 1978
$SO_2 + H_2O \rightleftharpoons HSO_3^- + H^+$	$3.13 \cdot 10^{-4}$	1940	Beilke and Gravenhorst, 1978
$HSO_3^- \rightleftharpoons SO_3^{2-} + H^+$	$6.22 \cdot 10^{-8}\ M$		Beilke and Gravenhorst, 1978
$HSO_3^- + CH_2(OH)_{2(aq)} \rightarrow HMS^-$	$0.436\ M^{-1}\ s^{-1}$	2990	Boyce and Hoffmann, 1984
$HMS^- \rightarrow HSO_3^- + CH_2(OH)_{2(aq)}$	$1.22 \cdot 10^{-7}\ s^{-1}$		[a]
$SO_3^{2-} + CH_2(OH)_{2(aq)} \rightarrow HMS^-$	$1.23 \cdot 10^5\ M^{-1}\ s^{-1}$	2450	Boyce and Hoffmann, 1984
$HMS^- \rightarrow SO_3^{2-} + CH_2(OH)_{2(aq)}$	$3.8 \cdot 10^{-6}\ s^{-1}$	5530	[b]
$CH_2(OH)_{2(aq)} + OH \rightarrow$ products	$1 \cdot 10^9\ M^{-1}\ s^{-1}$	1020	Chin and Wine , 1994
$HSO_3^- + H_2O_2 + H^+ \rightarrow$ products	$7.2 \cdot 10^7\ M^{-2}\ s^{-1}$	4000	Betterton and Hoffmann, 1988
$HSO_3^- + O_3 \rightarrow$ products	$3.7 \cdot 10^5\ M^{-1}\ s^{-1}$	5530	Hoffmann, 1986
$SO_3^{2-} + O_3 \rightarrow$ products	$1.5 \cdot 10^9\ M^{-1}\ s^{-1}$	5280	Hoffmann, 1986
$HMS^- + OH \rightarrow HSO_3^- + HCOOH$	$3 \cdot 10^8\ M^{-1}\ s^{-1}$		Barlow *et al.*, 1997

[a] Calculated based on the rate constant for the forward reaction and the equilibrium constant given by Olson and Hoffmann.
[b] k^{1st} at pH = 7, extrapolated from the data by Kok *et al.*, 1986.

overestimation of the HMS^- concentration, other sinks for sulfur(IV), i.e., the oxidation by H_2O_2 and O_3, were considered in the model.

As can be seen in Figure 4 OH reaction with formaldehyde will not influence the equilibrium formaldehyde concentration in the droplet since the timescale for the chemical reaction is longer than those for the other processes. But the ratio might be affected by HMS^- formation, since HMS^- formation leads to a higher apparent solubility of formaldehyde in the aqueous phase. As mentioned above, the pure uptake model applied to formaldehyde predicts the same concentration in both droplet classes after a few seconds (ratio = 1).

The effective solubility for formaldehyde is increased if HMS^- is formed. The partitioning at equilibrium can be described as

$$\begin{aligned} K_H^{\text{eff, HMS}}(HCHO) &= \frac{HCHO_{aq} + HMS^-}{HCHO_g} \\ &= K_H^{\text{eff}}(HCHO) \cdot (1 + K^{HMS} \cdot [S(IV)]_{aq})\ [M\ atm^{-1}] \end{aligned} \tag{17}$$

with $K^{HMS} = [HMS^-]/([S(IV)]_{aq} \cdot [HCHO]_{aq})$. Therefore, the solubility of formaldehyde depends on the concentration of sulfur(IV). As shown in Figure 4 the time scale for the uptake of acids depends on the pH. The effective Henry's Law Constant for SO_2 at pH = 7 is $K_H^{\text{eff}}(S(IV)) = 10^6\ M\ atm^{-1}$ being comparable to that of acetic acid. It implies that SO_2 might show a similar uptake time scale as this acid. The HMS^- formation and finally the increase of the total formaldehyde

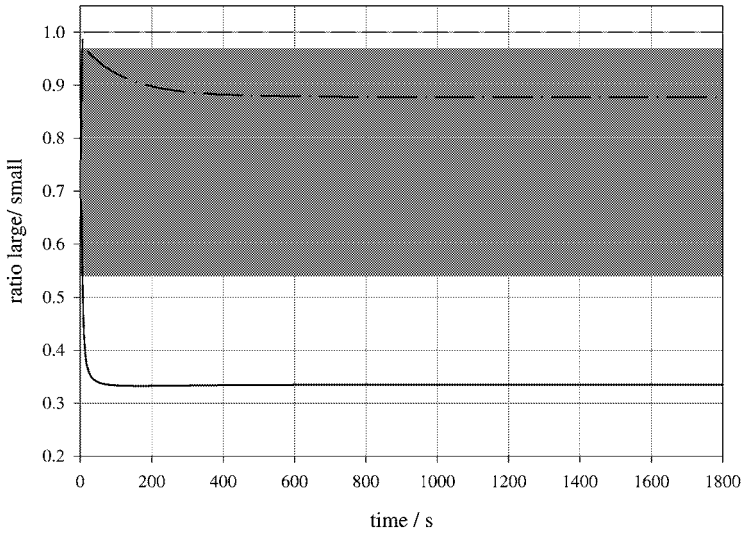

Figure 7. Concentration ratios for formaldehyde – – – – no HMS-formation, — · — · ; with HMS^- formation (pH = 7), shadowed area: measured ratios (average ± standard deviation); $[S(IV)]_{aq}/[HCHO_{tot}]_{aq} = 0.2$ (small droplets), $[S(IV)]_{aq}/[HCHO_{tot}]_{aq} = 0.1$ large droplets; ——— with HMS^- formation at high concentration of SO_2 (= lower limit for concentration ratio for formaldehyde).

concentration in the droplet are correlated with the concentration and the mass transfer rate of SO_2.

A few concentration values are available from the observations for sulfur(IV) concentrations in large and small droplets, respectively (≈ 3 μeq/L in large droplets and ≈ 10 μeq/L in small droplets). Hence, the concentration ratio of $[S(IV)_{tot}]_{aq}/[HCHO_{tot}]_{aq}$ in the droplets (referring to the total concentrations, i.e. considering the HMS^- concentration for both species, respectively) is about 0.2 in the small and 0.1 in the large droplets. At the high pH values found in the fog drops the formation of HMS^- is fairly rapid, about six orders of magnitude faster than at low pH (Table V). Therefore, at low total sulfur(IV) concentrations HMS^- formation is limited by the available sulfur(IV). In order to estimate the extent to which HMS^- formation might influence the concentration ratio of formaldehyde in the droplets under such conditions, an initial $SO_{2(g)}$ concentration was chosen leading to a sulfur(IV)/HCHO ratio in the aqueous phase comparable to the observed ratios. Figure 7 shows that the concentration ratio for formaldehyde is decreased to about 0.88. Comparison with the measured values shows that concentration ratios of formaldehyde between 0.45 and 0.95 were observed. Hence, the model approach confirms a decreased concentration ratio for formaldehyde due to HMS^- formation but predicts a smaller effect than observed in the fog drops.

More generally, it can be estimated under which conditions the HMS^- formation might have the largest influence on the concentration ratio of formaldehyde: if the SO_2 aqueous phase concentration is completely controlled by transport

processes, i.e., if the deviation from the equilibrium concentration ($p_A - c_{aq}/K_H^{eff}$) (Equation (6)) is about the same in both drop size classes, the change in the aqueous phase concentrations is determined only by the mass transfer coefficient k_{mt} of SO_2. Thus, the aqueous phase concentration ratio of formaldehyde corresponds then to the ratio of k_{mt} for small and large droplets, respectively. Assuming values for SO_2 of $D_g = 10^{-5}$ m^2 s^{-1}, $\alpha = 0.05$, $c = 500$ m s^{-1} we can calculate a ratio of $k_{mt}(SO_2)_{large}/k_{mt}(SO_2)_{small} = 0.3$.

Hence, this value represents the lower limit for the concentration ratio for formaldehyde but it can only be achieved if the SO_2 concentration is sufficiently high and the HMS^- formation is not controlled by the concentration ratio of [S(IV)]/[HCHO] in the drops.

Improved input data sets, not only of sulfur(IV) concentrations, but also for other species as considered in the chemistry model, such as SO_2 and OH, might produce better agreement between the measured and modeled values.

3.4. MIXING EFFECTS

3.4.1. *Definition*

As discussed in previous studies (e.g., Pandis and Seinfeld, 1991) the mixing of individual droplets into a bulk sample can lead to a different concentration than the average value present in the original droplets. It was shown that the concentrations of solutes (NH_3, SO_2) in a bulk sample always exceed the concentrations predicted by thermodynamic equilibrium, even if individual drops are in equilibrium. This effect is caused by the change in the average pH value that occurs when single droplets are combined into a bulk sample. The situation becomes more complicated if buffering effects occur due to interactions of different acidic or basic species within the bulk samples. In several studies buffering effects were explained by inorganics such as ammonia, nitrate, carbonate and sulfate. Additionally significant contributions to buffering, perhaps by organics, were found at $4 < pH < 7$ in California fogs (Collett *et al.*, 1999b). In the following discussion such buffering effects will not be considered. This assumption represents an oversimplification but it allows an estimate of the potential impact of mixing effects.

In order to estimate the extent to which mixing effects can explain the observed concentration patterns, one of the measured droplet number distributions was chosen (Figure 8(a)). Because there is no clear trend regarding the pH values within the droplet distribution, three different extreme pH distributions were assumed, differing between pH = 6.5 and 7.5 in both the small and large droplets (Figure 8(b), bottom). The first distribution (I) assumes a monotonically increasing pH value from the smallest to largest drop size in each class; the second distribution (II) describes a monotonically decreasing pH value. The third distribution contains a maximum pH value in the middle drop size class. These pH distributions cover the limits of the pH variability determined in the study. Furthermore it is assumed that

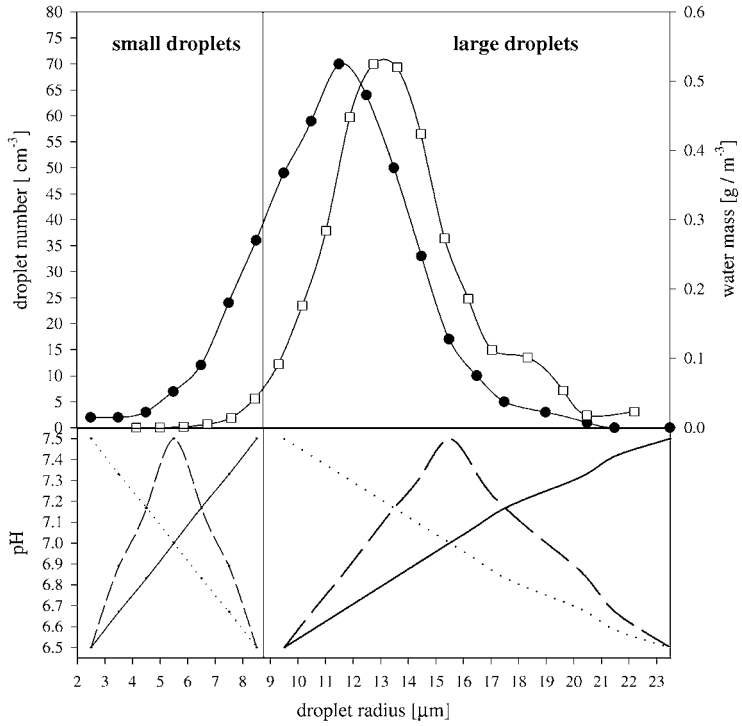

Figure 8. Droplet number distribution (●), water mass distribution (□) and pH values (bottom part) used for Equations (18)–(20), solid line: I; dotted line: II, broken line: III.

– despite the previous discussion – the individual droplets were in thermodynamic equilibrium.

3.4.2. *Calculation of the Acid Concentration in Individual Droplets and the Bulk Sample*

The theoretical equilibrium acid concentrations $c_{\mathrm{aq},i}$ in all individual droplets can be derived from the corresponding effective Henry's Law constants for the H^+ concentrations $[H^+]_i$ (Figure 8(b))

$$c_{\mathrm{aq},i} = c_g \cdot \left[\mathrm{K_H} \cdot \left(1 + \frac{\mathrm{K}_a}{[\mathrm{H}^+]_i} \right) \right] \tag{18a}$$

with $\mathrm{K_H}$ and K_a given in Table III. For the calculations gas phase concentrations of $c_g = 0.1$ ppb for both formic and acetic acid were assumed. The sum of the concentrations $c_{\mathrm{aq},i}$ multiplied by the corresponding volume fraction of the liquid water gives the total acid concentration $c_{\mathrm{aq},i,\mathrm{sum}}$.

$$c_{\mathrm{aq},i,\mathrm{sum}} = \frac{c_{\mathrm{aq},i} \cdot \mathrm{V}_i}{\Sigma(\mathrm{V}_i)}. \tag{19}$$

The concentration obtained by (19) represents the sum of all moles of the species in all droplets. This approach is adequate for pH independent species but neglects the pH dependence of the acid solubility.

The average pH in the bulk sample is calculated as a volume weighted average (analogous to Equation (18a)). This average H^+ concentration is used to calculate the equilibrium acid concentration in the bulk sample ($c_{\text{aq, sample}}$)

$$c_{\text{aq, sample}} = c_g \cdot \left[\mathrm{K_H} \cdot \left(1 + \frac{\mathrm{K}_a}{[\mathrm{H}^+]_{\text{sample}}} \right) \right]. \tag{18b}$$

The ratio S of the concentrations obtained by Equations (18a) and (18b) shows whether the collected samples should be sub- or supersaturated with regards to the acid concentrations assuming equilibrium in the individual droplets.

$$S = \frac{c_{\text{aq},i,\text{sum}}}{c_{\text{aq, sample}}}. \tag{20}$$

Table VI shows these S values calculated from (20) for all three assumed pH distributions and both acids. According to (20) a value of S greater than 1 shows that the total amount of acid in the individual droplets ($c_{\text{aq},i,\text{sum}}$) was larger than that in the corresponding combined sample ($c_{\text{aq, sample}}$). In fact, all values of S are greater than 1; this means that by combining the individual droplets into bulk samples, some of the acid might evaporate. The comparison of the values for large and small droplets in Table VI shows a slight tendency to higher concentration deviations between $c_{\text{aq, sample}}$ and $c_{\text{aq},i,\text{sum}}$ in large droplets. Therefore, the evaporation rate from these samples might be higher and thus the large/small drop ratio measured based on the acid concentration in the bulk samples might be too small. These deviations are roughly $<15\%$ for all cases assumed here as can be seen from the comparison of the different ratios in Table VI ($c^{\text{large}}_{\text{aq, sample}}/c^{\text{small}}_{\text{aq, sample}}$ vs. $c^{\text{large}}_{\text{aq},i,\text{sum}}/c^{\text{small}}_{\text{aq},i,\text{sum}}$). It is likely that this artifact is even smaller than estimated here because the evaporation rate from the collected sample will be delayed after a certain collection period due to the saturation of the gas phase with acid vapor above the collection bottle. Furthermore, the surface area/volume ratio decreases once the drops are combined also causing outgassing to be slowed from the bulk sample. Internal buffering in drop mixtures will also reduce this effect.

The above calculation represents a rough estimate of the possible influence of mixing effects. To give a more general picture more detailed size resolved measurements are necessary. The correlation between solubility and pH dependence is most sensitive at high pH, i.e., in that regime where the factor $K_a/[H^+]$ is greater than unity and determines K_H^{eff} (2). Therefore, it can be concluded that in droplets with lower pH values, i.e., closer to the K_a values of the acids, the mixing effects will have an even smaller impact than estimated here.

Table VI. Calculated supersaturations S (Equation (20)) for small (<8.5 μm) and large droplets (>8.5 μm) and concentration ratios in individual droplets (Equation (18a)) and combined bulk samples (Equation (18b)), corresponding to assumed pH distributions I–III (Figure 8)

pH	I		II		III	
	S					
distribution	Large droplets	Small droplets	Large droplets	Small droplets	Large droplets	Small droplets
HCOOH	1.25	1.12	1.28	1.13	1.48	1.44
CH_3COOH	1.2	1.13	1.28	1.12	1.48	1.44
	Ratio					
	Bulk sample	Individual droplets	Bulk sample	Individual droplets	Bulk sample	Individual droplets
HCOOH	0.27	0.3	3.29	3.76	2.12	2.17
CH_3COOH	0.28	0.3	3.28	3.73	2.11	2.09

4. Conclusions

Small chain carboxylic acids and formaldehyde are major components of the total organic carbon in fog droplets. While acetic acid, the single most abundant organic compound, may account for up to 22% of the TOC, dicarboxylic acids (mostly oxalic acid) were only minor components of the TOC ($\leqslant 2\%$). Size-resolved measurements of organic acids showed a clear heterogeneity in concentrations between small ($r < 8.5$ μm) and large ($r > 8.5$ μm) droplets, with the small droplets typically being more concentrated. For non-volatile species like oxalic acid this result is consistent with preferential enrichment in small cloud condensation nuclei. For volatile species like formaldehyde and formic and acetic acid, the origin of the heterogeneity has been investigated using an uptake model.

In some cases application of Henry's Law to predict the partitioning of the acids is sufficient, if the pH dependence of the acid solubility or hydration of formaldehyde is considered. For example, formaldehyde might achieve thermodynamic equilibrium in the droplet after a few seconds. Comparing time scales for the transport towards the droplet it becomes evident that the time until saturation for formic acid is about a factor of 10 greater than the corresponding time for acetic acid. This implies that, for sufficiently long drop life times, the ratio of acetic acid concentrations is likely to be closer to 1, i.e., closer to equilibrium.

The possible impact of chemical reactions, in particular oxidation by OH, on the species concentrations in small and large droplets was investigated. These effects are highly sensitive to the assumed OH concentration. It is expected that at low OH concentrations ('nighttime') this impact will be negligible but at high OH

concentrations ('daytime') the concentrations can be influenced significantly. The departure from equilibrium will be larger in large droplets so that the large/small droplet concentration ratio will decrease. Considering the formation of hydroxymethanesulfonate, uptake of formaldehyde can be enhanced. Depending on the sulfur(IV) concentration the measured formaldehyde concentrations (including hydroxymethanesulfonate) can be higher than predicted by Henry's Law. Due to the high solubility of S(IV) at high pH values its uptake rate will be different for different droplet size classes. Thus, HMS formation leads to a decrease in the concentration ratio for formaldehyde in the cases considered here.

The influence of possible artifacts by mixing effects was investigated. It has been shown that these effects might lead to an underestimation of the ratio of large-to-small drop concentrations because potential supersaturation and evaporation are larger in the large droplet sizes. It was estimated that in total such effects will lead to deviations of $<15\%$ from the ratio present originally in the individual droplets.

With the current model study it is concluded that concentration heterogeneities in fog droplets are produced by the high effective solubility of the species and correspondingly long times to achieve phase equilibrium, due to the limited lifetime of the fog droplets. Concentration heterogeneities can also be affected by concentrations of reactants (e.g., OH) in the aqueous phase. These findings are in agreement with conclusions of other studies. In several studies it was assumed that drop size dependent concentrations in fog and cloud droplets might be caused by kinetic inhibition of mass transfer (e.g., Winiwarter *et al*., 1994). While in these previous studies these effects were not investigated numerically in the present study bounds are given for each of the possible limitations. Thus, the model applied here enables a prediction of the partitioning of the volatile species investigated in this study (formic acid, acetic, acid, and formaldehyde) and might even be extended to other compounds. In the future, more complete datasets, including measurements with high temporal resolution of gas phase concentrations of low molecular weight organic compounds, should enhance our understanding of the drop-size dependent concentrations of volatile species.

Acknowledgements

We are grateful to E. Sherman for his contributions to the design of the new stainless steel collectors and for assistance in the preparation of the field project. We are grateful to J. Reilly, G. Kang, H. Chang. and S. Emert for assistance during the field experiment. This work was supported in part by the NOAA Office of Global Programs. This work was also funded in part by the National Science Foundation (ATM-9980540, ATM-0222607) and the San Joaquin Valleywide Air Pollution Study Agency. The statements and conclusions in this report are those of the Contractor and not necessarily those of the California Air Resources Board, the San Joaquin Valleywide Air Pollution Study Agency, or its Policy Committee, their employees or their members. The mention of commercial products, their source, or

their use in connection with material reported herein is not to be construed as actual or implied endorsement of such products.

References

Ang, C. C., Lipari, F., and Swarin, S., 1987: Determination of hydroxymethanesulfonate in wet deposition samples, *Environ. Sci. Technol.* **21**, 102–105.

Audiffren, N., Renard, M., Buisson, E., and Chaumerliac, N., 1998: Deviations from the Henry's Law equilibrium during cloud events: A numerical approach of the mass transfer between phases and its specific numerical effects, *Atmos. Res.* **49**, 139–161.

Barlow, S., Buxton, G. V., Murray, S. A., and Salmon, G. A., 1997: Free-radical-induced oxidation of hydroxymethanesulfonate in aqueous solution, Part 1: A pulse radiolysis study of the reactions of OH and SO_4^-, *J. Chem. Soc. Faraday Trans.* **93** (20), 3637–3640.

Bator, A. and Collett Jr., J. L., 1997: Cloud chemistry varies with drop size, *J. Geophys. Res.* **102**, 28071–28078.

Beilke, S. and Gravenhorst, G., 1978: Heterogeneous SO_2-oxidation in the droplet phase, *Atmos.Environ.* **12**, 231–239.

Betterton, E. A. and Hoffmann, M. R., 1988: Oxidation of aqueous SO_2 by peroxymonosulfate, *J. Phys. Chem.* **92**, 5962–5965.

Boyce, S. D. and Hoffmann, M. R., 1984: Kinetics and mechanism of the formation of hydroxymethane-sulfonic acid at low pH, *J. Phys. Chem.* **88**, 4740–4746.

Chin, M. and Wine, P. H., 1994: A temperature-dependent competitive kinetics study of the aqueous-phase reactions of OH radicals with formate, formic acid, acetate, acetic acid and hydrated formaldehyde, in G. R. Helz, R. G. Zepp, and D. G. Crosby (ed.), *Aquatic and Surface Photochemistry*, Lewis Publishers, Boca Raton, pp. 85–96.

Collett Jr., J. L., Bator, A., Rao, X., and Demoz, B. B., 1994: Acidity variations across the cloud drop size spectrum and their influence on rates of atmospheric sulfate production, *Geophys. Res. Lett.* **21**, 2393–2396.

Collett Jr., J. L., Hoag, K. J., Sherman, D. E., Bator, A., and Richards, L. W., 1999a: Spatial and temporal variations in San Joaquin Valley fog chemistry, *Atmos. Environ.* **33**, 129–140.

Collett Jr., J. L., Hoag, K. J., Rao, X., and Pandis, S. N., 1999b: Internal buffering in San Joaquin Valley fog drops and its influence on aerosol processing, *Atmos. Environ.* **33**, 4833–4847.

Davidovits, M., Hu, J. H., Worsnop, D. R., Zahniser, M. S., and Kolb, C. E., 1995: Entry of gas molecules into liquids, *Faraday Discuss.* **100**, 65–82.

Demoz, B. B., Collett Jr., J. L., and Daube Jr., B. C., 1996: On the design and performance of the California institute of technology cloudwater collector, *Atmos. Res.* **41**, 47–62.

Dong, S. and Dasgupta, P. K., 1987: Fast fluorimetric flow-injection analysis of formaldehyde in atmospheric water, *Environ. Sci. Technol.* **21**, 581–588.

Ervens, B., Williams, J., Buxton, G. V., Salmon, G. A., Bydder, M., Dentener, F., George, C., Mirabel, P., Wolke, R., and Herrmann, H., 2003: CAPRAM2.4 (MODAC mechanism): An extended and condensed tropospheric aqueous phase mechanism and its application, *J. Geophys. Res.* **108**, D14 4426_doi: 10.1029/2002 JD002202.

Facchini, M. C., Lind, J., Orsi, G., and Fuzzi, S., 1990: The chemistry of carbonyl compounds in the Po Valley fog water, *Sci. Total Environ.* **91**, 79–86.

Feingold, G. and Chuang, P. Y., 2002: Analysis of the influence of film-forming compounds on droplet growth: Implications for cloud microphysical processes and climate, *J. Atmos. Sci.* **59**, 2006–2018.

Fuller, E. N., 1986: Diffusion coefficients for binary gas systems at low pressures: Empirical correlations, in C. Reid *et al.* (eds), *Properties of Gases and Liquids*, McGraw Hill, New York, p. 587.

Gill, P. S., Graedel, T. E., and Weschler, C. J., 1983: Organic films on atmospheric aerosol particles, fog droplets, cloud droplets, raindrops, and snow flakes, *Rev. Geophys. Space Phys.* **21**, 903–920.

Hanson, D., Burkholder, J. B., Howard, C. J., and Ravishankara, A. R., 1992: Measurement of OH and HO_2 radical uptake coefficients on water and sulfuric acid surfaces, *J. Phys. Chem.* **96**, 4979–4985.

Harned, H. S. and Owen, B. B., 1958, *The Physical Chemistry of Electrolytic Solutions* (3rd edn), Reinhold, New York.

Hegg, D. A., Gao, S., and H. Jonsson, 2002: Measurements of selected dicarboxylic acids in marine cloud water, *Atmos. Res.* **62**, 1–10.

Herckes, P., Lee, T., Trenary, L., Kang, G., Chang, H., and Collett Jr., J. L., 2002a: Organic matter in San Joaquin Valley radiation fogs, *Environ. Sci. Technol.* **36**, 4777–4782.

Herckes, P., Hannigan, M. P., Trenary, L., Lee, T., and Collett Jr., J. L., 2002b: Organic compounds in radiation fogs in Davis (California), *Atmos. Res.* **64**, 99–108.

Herrmann, H., Ervens, B., Jacobi, H.-W., Wolke, R., Nowacki, P., and Zellner, R., 2000: CAPRAM2.3: A chemical aqueous phase radical mechanism for tropospheric chemistry, *J. Atmos. Chem.* **36**, 231–284.

Hoffmann, M. R., 1986: On the kinetics and mechanism of oxidation of aquated sulfur dioxide by ozone, *Atmos. Environ.* **20**, 1145–1154.

Huthwelker, T. and Peter, T., 1996: Analytical description of gas transport across an interface with coupled diffusion in two phases, *J. Chem. Phys.* **105**, 1661–1667.

Jacob, D. J., 1986: Chemistry of OH in remote clouds and its role in the production of formic acid and peroxymonosulfate, *J. Geophys. Res.* **91**, 9807–9826.

Keene, W. C., Mosher, B. W., Jacob, D. J., Munger, J. W., Talbot, R. W., Artz, R. S., Maben, J. R., Daube Jr., B.C., and Galloway, J. N., 1995: Carboxylic acids in clouds at a high-elevation forested site in central Virginia, *J. Geophys. Res.* **100**, 9345–9357.

Khan, I. and Brimblecombe, P., 1992: Henry's Law constants of low molecular weight ($<$130) organic acids, *J. Aerosol Sci.* **23**, S897–S990.

Khare, P., Kumar, N., Kumari, K. M., and Srivastava, S. S., 1999: Atmospheric formic and acetic acids: An overview, *Rev. Geophys.* **37**, 227–248.

Khwaja, H., A., Brudnoy, S., and Husain L., 1995: Chemical characterization of three summer cloud episodes at Whiteface Mountain, *Chemosphere* **31**, 3357–3381.

Kläning, U. K., Sehested, K., and Holcman, J., 1985: Standard Gibbs energy of formation of the hydroxyl radical in aqueous solution. Rate constants for the reaction $ClO_2^- + O_3 = O_3^- + ClO_2$, *J. Phys. Chem.* **89**, 760–763.

Klippel, W. and Warneck, P., 1980: The formaldehyde content of the atmospheric aerosol, *Atmos. Environ.* **14**, 809–818.

Kok, G. L., Gitlen, S. N., and Lazrus, A. L., 1986: Kinetics of the formation and decomposition of hydroxymethanesulfonate, *J. Geophys. Res.* **91**, 2801–2804.

Laj, P., Fuzzi, S., Lazzari, A., Ricci, L., Orsi, G., Berner, A., Dusek, U., Schell, D., Guenther, A., Wendisch, M., Wobrock, W., Frank, G., Martinsson, B., and Hillamo, R., 1998: The size-dependent chemistry of fog droplets, *Contrib. Atmos. Phys.* **71**, 115–130.

Leriche, M., Voisin, D., Chaumerliac, N., Monod, A., and Aumont, B., 2000: A model for tropospheric multiphase chemistry: Application to one cloudy event during the CIME experiment, *Atmos. Environ.* **34**, 5015–5036.

Lide, D. R. (ed.), 2000: *Handbook of Chemistry and Physics* (81st edn), CRC Press, New York.

Löflund, M., Kasper-Giebl, A., Schuster, B., Giebl, H., Hitzenberger, R., and Puxbaum, H., 2002: Formic, acetic, oxalic, malonic and succinic acid concentrations and their contribution to organic carbon in cloud water, *Atmos. Environ.* **36**, 1553–1558.

Ludwig, J., and Klemm, O., 1988: Organic acids in different size classes of atmospheric particulate material, *Tellus* **40B**, 340–347.

Millet, M., Sanusi, A., and Wortham, H., 1996: Chemical composition of fogwater in an urban area: Strasbourg (France), *Environ. Poll.* **94**, 345–354.

Millet, M., Wortham, H., Sanusi, A., and Mirabel, P., 1997: Low-molecular-weight organic-acids in fogwater in an urban area – Strasbourg (France), *Sci. Total Environ.* **206**, 57–65.

Munger, J. W., Collett, Jr., J. L., Daube Jr., B., and Hoffmann, M. R., 1989a: Carboxylic acids and carbonyl compounds in southern California clouds and fogs, *Tellus* **41B**, 230–242.

Munger, J. W., Collett Jr., J. L., Daube Jr., B., and Hoffmann, M. R., 1989b: Chemical composition of coastal stratus clouds: Dependence on droplet size and distance from the coast, *Atmos. Environ.* **23**, 2305–2320.

Munger, J. W., Collett Jr., J. L., Daube Jr., B., and Hoffmann, M. R., 1990: Fogwater chemistry at Riverside, California. *Atmos. Environ.* **24B**, 185–205.

Nathanson, G. M., Davidovits, P., Worsnop, D. R., and Kolb, C. E., 1996: Dynamics and kinetics at the gas-liquid interface, *J. Phys. Chem.* **100**, 13007–13020.

Neusüß, C. Pelzing, M., Plewka, A., and Herrmann, H., 2000: A new analytical approach for size-resolved speciation of organic compounds in atmospheric aerosol particles: Methods and first results, *J. Geophys. Res.* **105**, 4513–4527.

Noone, K. J., Ogren, J. A., Hallberg, A., Heintzenberg, J., Hansson, H.-C., Svenigsson, I. B., Wiedensohler, A., Fuzzi, S., Facchini, M. C., Arends, B. G., and Berner, A., 1992: Changes in aerosol size- and phase distributions due to physical and chemical processes in fog, *Tellus* **44B**, 489–504.

Ogren, J. A. and Charlson, R. J., 1992: Implications for models and measurements of chemical inhomogeneities among cloud droplets, *Tellus* **44B**, 208–225.

Ogren, J. A., Noone, K. J., Hallberg, A., Heintzenberg, J., Schell, D., Berner, A., Solly, I., Kruisz, C., Reischl, G., Arends, B. G., and Wobrock, W., 1992: Measurements of the size dependence of the concentration of non-volatile material in fog droplets, *Tellus* **44B**, 570–580.

Olson, T. M. and Hoffmann, M. R., 1989: Hydroxyalkylsulfonate formation: Its role as a S(IV) reservoir in atmospheric water droplets, *Atmos. Environ.* **23**, 985–997.

Pandis, S. N., Seinfeld, J. H., and Pilinis, C., 1990: Chemical composition differences in fog and cloud droplets of different sizes, *Atmos. Environ.* **24A**, 1957–1969.

Pandis, S. N. and Seinfeld, J. H., 1991: Should bulk cloudwater or fogwater samples obey Henry's Law?, *J. Geophys. Res.* **96**, 10791–10798.

Podzimek, J. and Saad, A. N., 1975: Retardation of condensation nuclei growth by surfactant, *J. Geophys. Res.* **80**, 3386–3392.

Reilly, J. E., Rattigan, O. V., Moore, K. F., Judd, C., Sherman, D. E., Dutkievicz, V. A., Kreidenweis, S. M., Husain, L., and Collett Jr., J. L., 2001: Drop size dependent S(IV) oxidation in chemically heterogeneous radiation fogs, *Atmos. Environ.* **35**, 5717–5728.

Saxena, P. and Hildemann, L. M., 1996: Water-soluble organics in atmospheric particles: A critical review of the literature and application of thermodynamics to identify candidate compounds, *J. Atmos. Chem.* **24**, 57–109.

Schwartz, S., 1986: Mass transport considerations pertinent to aqueous phase reactions of gases in liquid water clouds, in Jaeschke, W. (ed.), *Chemistry of Multiphase Atmospheric Systems*, NATO ASI Series, Springer, Berlin, pp. 415–471.

Swartz, E., Boniface, J., Tchertkov, I., Rattigan, O. V., Robinson, D. V., Davidovits, P., Worsnop, D. R., Jayne, J. T., and Kolb, C. E., 1997: Horizontal bubble train apparatus for heterogeneous chemistry studies: Uptake of gas phase formaldehyde, *Environ. Sci. Technol.* **37**, 2634–2641.

Voisin, D., Legrand, M., and Chaumerliac, N., 2000: Scavenging of acidic gases (HCOOH, CH_3COOH, HNO_3, HCl and SO_2) and ammonia in mixed liquid-solid water clouds at the Puy de Dôme mountain (France), *J. Geophys. Res.* **105**, 6817–6835.

Warneck, P., 1999: The relative importance of various pathways for the oxidation of sulfur dioxide and nitrogen dioxide in sunlit continental fair weather clouds, *Phys. Chem. Chem. Phys.* **1**, 5471–5483.

Winiwarter, W., Puxbaum, H., Facchini, M. C., Orsi, G., Beltz, N., Enderle, K., and Jaeschke, W., 1988: Organic acid gas and liquid-phase measurements in Po Valley fall-winter conditions in the presence of fog, *Tellus* **40B**, 348–357.

Winiwarter, W., Fierlinger, H., Puxbaum, H., Facchini, M. C., Arends, B. G., Fuzzi, S., Schell, D., Kaminski, U., Pahl, S., Schneider, T., Berner, A., Solly, I., and Kruisz, C., 1994: Henry's Law and the behavior of weak acids and bases in fog and clouds, *J. Atmos. Chem.* **19**, 173–188.

Worsnop, D. R., Morris, J. W., Shi, Q., Davidovits, P., and Kolb, C. E., 2002: A chemical kinetic model for reactive transformations of aerosol particles, *Geophys. Res. Lett.* **29** (20), 1996.

Wortham, H., Millet, M., Sanusi, A., and Mirabel, P., 1995: Methods of sampling, preservation and analysis of organic acids in atmospheric samples: A review, *Analysis* **23**, 427–436.

Yao, X., Fang, M., and Chan, C. K., 2002: Size distributions and formation of dicarboxylic acids in atmospheric particles, *Atmos. Environ.* **36**, 2099–2107.

Yu, S., 2000: Role of organic acids (formic, acetic, pyruvic and oxalic) in the formation of cloud condensation nuclei (CCN): A review, *Atmos. Res.* **53**, 185–217.